

Composite Cathodes with Succinonitrile-Based Ionic Conductors for Long-Cycle-Life Solid-State Lithium Metal Batteries

Chengzhou Xin,^[a] Kaihua Wen,^[a] Chuanjiao Xue,^[a] Shuo Wang,^[a] Ying Liang,^[a] Xinbin Wu,^[a] Liangliang Li,^{*[a]} and Ce-Wen Nan^[a]

Poor interfacial contacts between cathode active materials and solid-state electrolytes in solid-state lithium (Li) metal batteries often lead to a poor Li-ion conductive pathway, and thus a short cycle life and a low energy density. In this work, we synthesized succinonitrile (SCN)-based ionic conductors (ICs) with different flowability at room temperature for using in the composite cathodes and investigated the effect of the ICs on the cycle performance of the solid-state Li metal batteries with a poly(vinylidene fluoride) (PVDF)-based polymer electrolyte

separator. Our results showed that the gel-like SCN-LiClO₄ IC was superior to the flowable SCN-LiTFSI [lithium bis(trifluoromethanesulfonyl)imide] IC and the rigid SCN-LiClO₄ IC. The gel-like IC can build an effective Li-ion conduction path in the cathodes, establish a stable cathode/electrolyte interface with a small interfacial resistance change during cycling, and allow a high mass loading of active materials, which enables a long cycle life and high energy density of solid-state batteries.

1. Introduction

Solid-state lithium metal batteries have recently been intensively investigated to improve the energy density and safety of Li-ion batteries, and meanwhile numerous works have been devoted to developing solid-state electrolytes with high ionic conductivity, wide electrochemical stability window and large Li-ion transference number.^[1–5] In solid-state batteries, solid-solid interfaces are critical challenges due to poor physical contact. It is critical to establish an intimate interface between a cathode and a solid-state electrolyte separator.^[6–8] Meanwhile, effective Li-ion and electronic conductive pathways are needed in a composite cathode.^[9–12]

Various methods have been developed to improve the interfaces between a composite cathode and a solid-state electrolyte separator, and between cathode active particles and the electrolyte within the composite cathode. For the batteries with an oxide solid electrolyte, the interfacial contact resistance between the cathode and the electrolyte separator is usually large and cracks may appear in the cathode.^[13–16] Therefore, various flexible, ionic conductive additives have been used to enhance the cycle performance of the batteries at room temperature (RT).^[17–22] For example, a curable polymer-based glue was applied between a Li_{6.75}La₃Zr_{1.75}Ta_{0.25}O₁₂ ceramic pellet and a cathode with sulfurized polyacrylonitrile and the all-solid-

state batteries with the glue modification showed significantly reduced impedance and exhibit stable cycling performance at RT.^[19] Recently, polymer-based electrolytes have attracted much attention due to their good processibility and suitability for commercial applications.^[23–29] The solid-solid interfaces on the cathode side in the batteries with a polymer electrolyte also need to be optimized to enhance the electrochemical performance of batteries.^[30–34] For instance, a composite cathode made of LiFePO₄ and super P was matched with a PEO-based composite electrolyte membrane in a solid-state battery and it is necessary to add a PVDF:SCN:LiClO₄ binder in the cathode to extend the cycle life of the battery at 60 °C.^[35]

The ionic conductor in the composite cathodes plays an important role in the cell performance since it can conduct Li ions and buffer the volume change of cathode active materials. Gel electrolytes and plasticizers as ionic conductors can be introduced to the composite cathodes to achieve a high mass loading of active materials.^[7,36–43] Among these additives, succinonitrile (SCN) has been widely used in the composite cathodes as ionic conductor to improve the battery performance.^[36–39] A high loading (10.5 mg cm⁻²) LiNi_{0.5}Co_{0.2}Mn_{0.3}O₂ composite cathode with SCN and lithium bis(trifluoromethanesulfonyl)imide (LiTFSI) was prepared and the assembled solid-state Li metal batteries showed a good capacity retention after 150 cycles at RT.^[38] A LiNi_{0.5}Co_{0.2}Mn_{0.3}O₂:PVDF:super P:SCN:LiTFSI composite cathode with a mass loading of 9–10 mg cm⁻² was used in a pouch cell with a Li_{6.75}La₃Zr_{1.75}Ta_{0.25}O₁₂-based 3D composite polymer electrolyte.^[39] However, in these works, some liquid electrolytes were still added to improve the interfacial contact. The effect of SCN-based ionic conductors in the composite cathodes on the cycle performance of polymer-based solid-state batteries without liquid electrolytes added has not been fully studied, and

[a] C. Xin, K. Wen, C. Xue, Dr. S. Wang, Y. Liang, X. Wu, Prof. L. Li, Prof. C.-W. Nan

State Key Laboratory of New Ceramics and Fine Processing, School of Materials Science and Engineering
Tsinghua University
Beijing 100084, China
E-mail: liliangliang@mail.tsinghua.edu.cn

 Supporting information for this article is available on the WWW under
<https://doi.org/10.1002/batt.202100162>

the cycle performance of these batteries needs to be further improved for practical applications.^[44]

In this work, we fabricated a solid-state Li metal battery with a SCN-based composite cathode and PVDF-based polymer electrolyte separator.^[45] To investigate the effect of the SCN-based ionic conductors on the cycle performance of the solid-state Li metal batteries, the SCN-based ionic conductors with different flowability at RT were used. The cells with a gel-like ionic conductor made of SCN and LiClO₄ showed a long cycle life, better than those of the cells with a flowable or rigid ionic conductor. In addition, the use of the gel-like ionic conductor enhanced the mass loading of active material in the composite cathode.

2. Results and Discussion

Raman spectroscopy was carried out to study the distribution of the SCN-based IC inside the cathode sheet after the redundant IC on the cathode surface was removed by a piece of absorbent paper. Four locations were randomly selected for each cathode sheet in the Raman tests. As shown in Figure 1(a–c), the four spectra of each cathode show similar patterns and the Raman peaks of SCN can be observed on every spectrum, indicating that the IC is evenly distributed inside the cathode for all three cases.^[46] Figure S2 (Supporting Information) shows the top-view SEM images and corresponding element distribution mapping of Cl and S of the LiCoO₂ composite cathode without SCN [Figure S2(a–c)] and the SCN-based composite cathodes with IC1 [Figures S2(d–f)], IC2 [Figure S2(g–i)] or IC3 [Figure S2(j–l)]. The SCN-based ICs cannot be observed on the IC1 and IC3-based composite cathodes by SEM [Figure S2(d, j), respectively], because the flowable and gel-like ICs flew away probably due to the thermal effect of the electron beam in SEM, whereas they can be clearly seen in the photographs as shown in Figure S3. In comparison, the SEM image of the IC2-based composite cathode shows a lot of SCN residue [Figure S2(g)], because the IC2 is rigid at RT and the exposure to the electron beam does not make it flowable. The strong intensity of the Cl signal originated from LiClO₄ in Figure S2(h) also demonstrates the existence of the IC2 in the cathode. In addition, the strong S signal originated from LiTFSI in Figure S2(f) indicates the existence of the IC1, although it is not clearly observed by SEM [Figure S2(d)].

The FTIR spectra of three kinds of ICs in Figure 2(a) show the main peaks of SCN at 762, 819, 918, 963, 1002, 1425 and

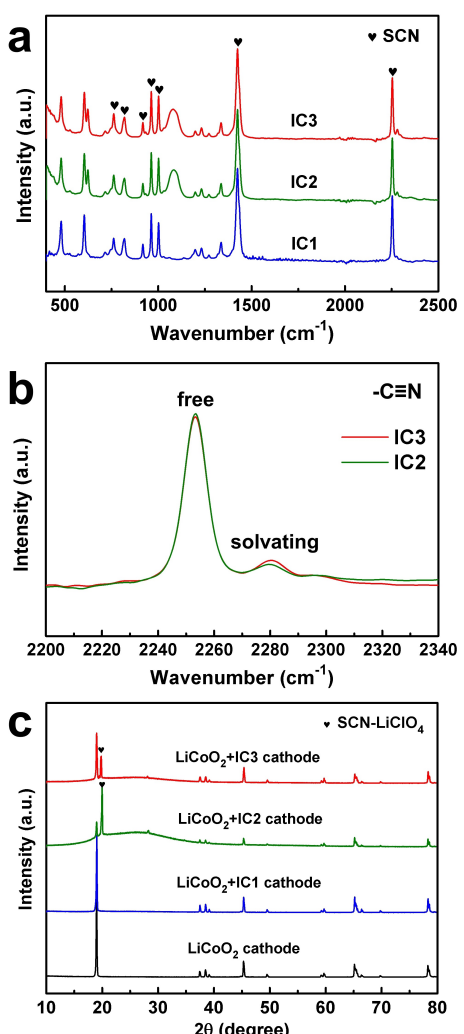


Figure 2. (a) FTIR spectra of three kinds of ICs. (b) FTIR spectra of the $-C\equiv N$ peaks of SCN in IC2 and IC3. (c) XRD patterns of the LiCoO₂ composite cathodes without SCN or with different ICs.

2253 cm⁻¹ are the same for three cases,^[47] indicating the structural consistency for these SCN-based ICs and no new substance generation comparing IC3 with IC2. The FTIR spectra of the $-C\equiv N$ peaks of SCN in IC2 and IC3 are compared in Figure 2(b). The peak intensity ratio of solvating SCN (2281 cm⁻¹) to free SCN (2253 cm⁻¹) for IC3 is larger than that for IC2, indicating more solvating SCN in IC3 due to the enhanced interaction between SCN and Li⁺.^[48] Figure 2(c)

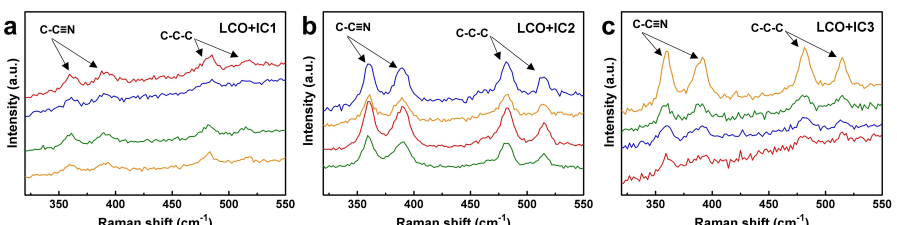


Figure 1. Raman spectra of the cathode sheets with (a) IC1, (b) IC2 or (c) IC3 at four randomly selected locations. LCO represents LiCoO₂.

shows XRD patterns of the LiCoO_2 composite cathodes without SCN or with three kinds of ICs. The positions of the peaks of the LiCoO_2 composite cathode do not change when the IC with LiTFSI or LiClO_4 is added to the cathode, indicating that there is no side reaction, and the SCN-based ICs are compatible with the cathode active materials. A new diffraction peak at $\sim 20^\circ$ appears for the cases of IC2 and IC3, which is originated from the crystalline structure of SCN- LiClO_4 .^[21,36] It is obvious that the cathode with gel-like IC3 has a weaker SCN- LiClO_4 peak in comparison with that containing rigid IC2, probably demonstrating a lower crystallinity for IC3,^[49] which is possibly attributed to the dissolution of more LiClO_4 in SCN with a long standing time and an extended heating time due to the solvation effect of SCN. In addition, the water contents in IC1, IC2 and IC3 were measured to be 0.86, 0.23 and 0.24 wt% by ^1H NMR (Figure S4), respectively. The water contents in IC2 and IC3 are almost the same. IC1 contains more water because it is easier for LiTFSI to absorb water than LiClO_4 .

The cycle performance and charge-discharge curves of the solid-state Li metal batteries with the SCN-based LiFePO_4 composite cathodes at a current density of 0.044 mA cm^{-2} are shown in Figure 3(a-d). The mass loading of LiFePO_4 active material is $1.5\text{--}2.0 \text{ mg cm}^{-2}$. The discharge capacity of the $\text{LiFePO}_4 + \text{IC1} || \text{PVDF-LiTFSI} || \text{Li}$ cell remains stable in the first 130 cycles and the corresponding capacity retention is 97.1% (142.9 mAh g^{-1} at the 1st cycle and 138.7 mAh g^{-1} at the 130th cycle with a C rate of 0.16 C). After 130 cycles, the capacity degrades quickly. In contrast, the $\text{LiFePO}_4 + \text{IC2} || \text{PVDF-LiTFSI} || \text{Li}$ cell shows a rapid capacity decay from the beginning of cycling with a C rate of 0.18 C, indicating that the rigid IC2 is not a good ionic conductor used to improve the cathode/electrolyte interface and establish desirable Li-ion pathways in the composite cathode. The $\text{LiFePO}_4 + \text{IC3} || \text{PVDF-LiTFSI} || \text{Li}$ cell shows a high cycling stability of 500 cycles with a capacity retention of 84.6% (154.3 mAh g^{-1} at the 1st cycle and 130.6 mAh g^{-1} at the 500th cycle with a C rate of 0.19 C), indicating that the use of the gel-like IC3 may reduce the

interfacial contact resistance between the cathode and the polymer electrolyte membrane and improve the Li-ion conduction in the cathode.

Figure 4 shows the cycle performance and charge-discharge curves of the LiCoO_2 batteries with various ICs in the cathodes at a current density of 0.044 mA cm^{-2} . The mass loading of active material is $1.4\text{--}2.3 \text{ mg cm}^{-2}$. The discharge capacity of the $\text{LiCoO}_2 + \text{IC1} || \text{PVDF-LiTFSI} || \text{Li}$ cell remains stable in the first 150 cycles (143.7 mAh g^{-1} at the 1st cycle and 135.3 mAh g^{-1} at the 150th cycle with a C rate of 0.18 C) and decays quickly in the following cycles. The capacity of the $\text{LiCoO}_2 + \text{IC2} || \text{PVDF-LiTFSI} || \text{Li}$ cell decays rapidly to $\sim 0 \text{ mAh g}^{-1}$ after 70 cycles with a C rate of 0.14 C. The cycle performance of the LiCoO_2 batteries with IC1 and IC2 is like that of the corresponding LiFePO_4 cells [Figure 3(a)]. In comparison, the $\text{LiCoO}_2 + \text{IC3} || \text{PVDF-LiTFSI} || \text{Li}$ cell shows a long cycle life. The discharge capacity retention after 285 cycles is 80.1% (129.9 mAh g^{-1} at the 1st cycle and 104 mAh g^{-1} at the 285th cycle with a C rate of 0.24 C). After 733 cycles, a discharge capacity of 36.6 mAh g^{-1} remains. The results of the cycle performance of both the LiFePO_4 and LiCoO_2 batteries show that IC3 is a good ionic conductor for using in the composite cathodes.

To analyze the origin for the decay of the batteries with the SCN-based ICs, electrochemical impedance spectroscopy (EIS) was carried out on the LiCoO_2 cells with three kinds of ICs before and after cycling and the results are shown in Figure 5. The equivalent circuit model for the EIS spectra in Figure 5 is shown in Figure S5. The intercept on the Z' -axis at high frequencies in the Nyquist plot represents the body resistance of the PVDF-LiTFSI electrolyte membrane R_b , while the suppressed semicircle at low frequencies represents the total interfacial resistance between the electrodes and the electrolyte R_i . The initial R_b is $8\text{--}10 \Omega$ and changes slightly after cycling ($12\text{--}24 \Omega$) for all three ICs. As for R_i , the values before cycling for the three batteries are similar and in the range of $42\text{--}85 \Omega$. Such a low R_i is much smaller than that of the batteries without

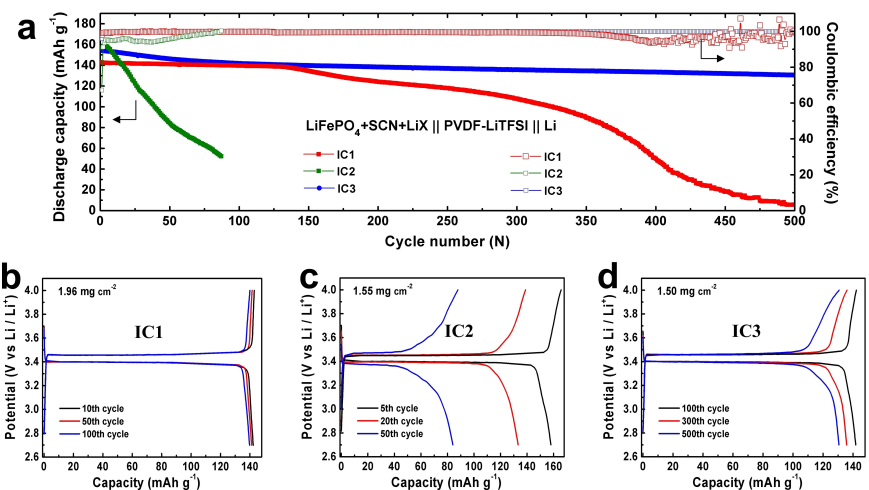


Figure 3. (a) Cycle performance of the $\text{LiFePO}_4 + \text{SCN} + \text{LiX} || \text{PVDF-LiTFSI} || \text{Li}$ batteries with various ICs and (b-d) corresponding charge-discharge curves of the batteries. LiX means LiTFSI or LiClO_4 . The mass loadings of LiFePO_4 active material are 1.96 , 1.55 and 1.50 mg cm^{-2} in (b-d), respectively.

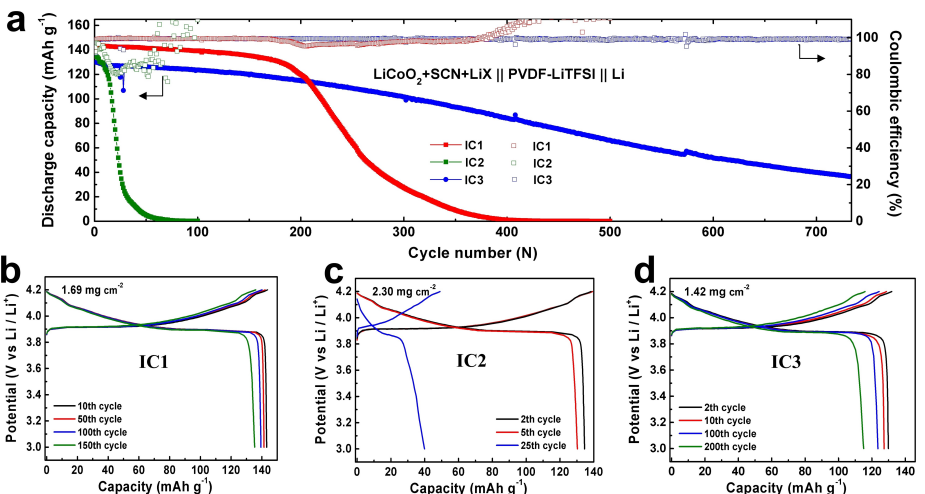


Figure 4. (a) Cycle performance of the $\text{LiCoO}_2 + \text{SCN} + \text{LiX} \parallel \text{PVDF-LiTFSI} \parallel \text{Li}$ batteries with various ICs and (b-d) corresponding charge-discharge curves of the batteries. LiX means LiTFSI or LiClO_4 . The mass loadings of LiCoO_2 active material are 1.69 , 2.30 and 1.42 mg cm^{-2} in (b-d), respectively.

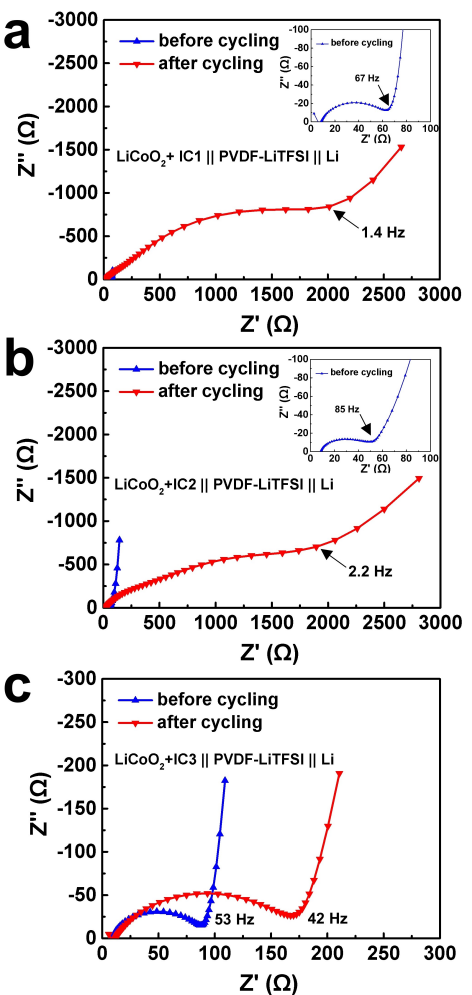


Figure 5. EIS spectra of the LiCoO_2 cells with (a) IC1, (b) IC2 or (c) IC3 before and after cycling. For (a) and (b), the EIS spectra after cycling were measured after the cells were charged/discharged for more than 500 and 100 cycles, respectively, where the discharge capacity was close to 0 mAh g^{-1} . For (c), the spectrum was taken after 734 cycles.

SCN ($\sim 2100 \Omega$)^[7] indicating that all three kinds of ICs are conducive for formation of good cathode/electrolyte interfacial contact before cycling. However, the R_i values of the batteries with IC1 and IC2 increase about two orders of magnitude up to ~ 2116 and 1750Ω after cycling, respectively, and the values of the corresponding interfacial resistance between the electrolyte and the composite cathode increase to ~ 1968 and 1424Ω according to the equivalent circuit model in Figure S5, respectively. In contrast, the R_i value of the battery with IC3 just increases to $\sim 163 \Omega$ after cycling. Therefore, it is likely that the degradation of the cathode/electrolyte interfaces during cycling is the main cause for the capacity decay of the batteries with IC1 and IC2 since the interfaces at the anode side are the same for these three cases.

The capacity of the cells with IC1 decays quickly after tens of cycles, which is because the liquid-like IC1 may flow away slowly during the long-term cycling, resulting in the disconnection of the Li-ion pathway and the increase of the cathode/electrolyte interfacial resistance.^[44] The Raman spectra of the composite cathode with IC1 after cycling are shown in Figure S6. No obvious Raman peak of SCN is observed, indicating that IC1 may flow away during cycling.

IC2 and IC3 show different flowability at RT due to different preparation procedures, though they have the same composition. Figure 6(a and b) shows the top-view SEM images of the LiCoO_2 cathodes with IC2 and IC3 after cycling, respectively, from which the cell with IC2 has cycled for more than 100 cycles with residue discharge capacity of $\sim 0.4 \text{ mAh g}^{-1}$ and the cell with IC3 has cycled for 290 cycles with remaining discharge capacity of 123.3 mAh g^{-1} . Micro-cracks are clearly observed in the composite cathode with IC2 after cycling, whereas the composite cathode with IC3 is still dense. Figure 6(c and d) shows the corresponding schematic diagrams of these cathodes. The rigid IC2 in the composite cathode may not accommodate the volume change of the active particles during repeated charge/discharge processes. In addition, the thickness of IC2 on the cathode/electrolyte interface cannot be

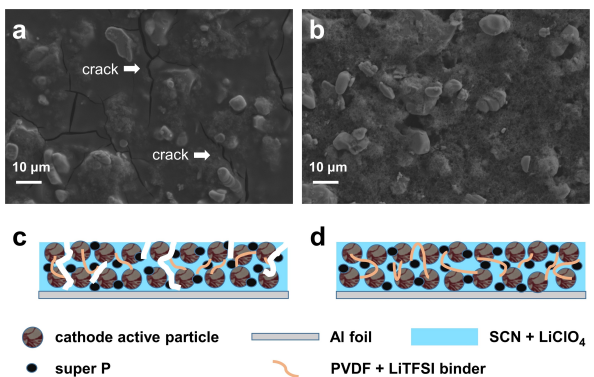


Figure 6. SEM images and schematic diagrams of the LiCoO_2 composite cathodes with (a, c) IC2 or (b, d) IC3 after cycling. The white lines in (c) represent cracks.

reduced by the applied pressure in the cell fabrication process and may act as a relatively thick rigid sheet on the cathode surface. Thus, the cracks appear, the interfacial resistance increases, and the cell performance degrades during cycling.

To test the electrochemical stability of IC3 against cathode active material during cycling, CV measurements were carried out on the LiFePO_4 and LiCoO_2 batteries with IC3. Figure 7(a and b) shows the CV curves of the $\text{LiCoO}_2 + \text{IC3} || \text{PVDF-LiTFSI} || \text{Li}$ cell and $\text{LiFePO}_4 + \text{IC3} || \text{PVDF-LiTFSI} || \text{Li}$ cells, respectively. For each case, the CV curves are well overlapped with each other after several cycles, indicating good electrochemical reversibility of the IC3-contained composite cathodes matched with the polymer electrolyte.

The gel-like IC3 was found to be a high-performance ionic conductor used in the cathode, based on the analysis above. Therefore, solid-state Li metal batteries with a high mass loading of the active materials were fabricated and tested. A $\text{LiFePO}_4 + \text{IC3} || \text{PVDF-LiTFSI} || \text{Li}$ cell with a mass loading of 6.05 mg cm^{-2} delivers an initial discharge capacity of 157.7 mAh g^{-1} at a current density of 0.044 mA cm^{-2} and a high-capacity retention of 92.9% after 160 cycles with a C rate of 0.05 C [Figure 8(a)]. A $\text{LiCoO}_2 + \text{IC3} || \text{PVDF-LiTFSI} || \text{Li}$ cell with a mass loading of 12.0 mg cm^{-2} can be cycled for 29 times at 0.03 C with a capacity retention of 92.6% [Figure 8(b)]. These results demonstrate that an effective Li-ion pathway is successfully established in both the composite cathodes with a high mass loading by adding the gel-like IC3. Table S1 compares the composite cathodes with different ionic conductors in the

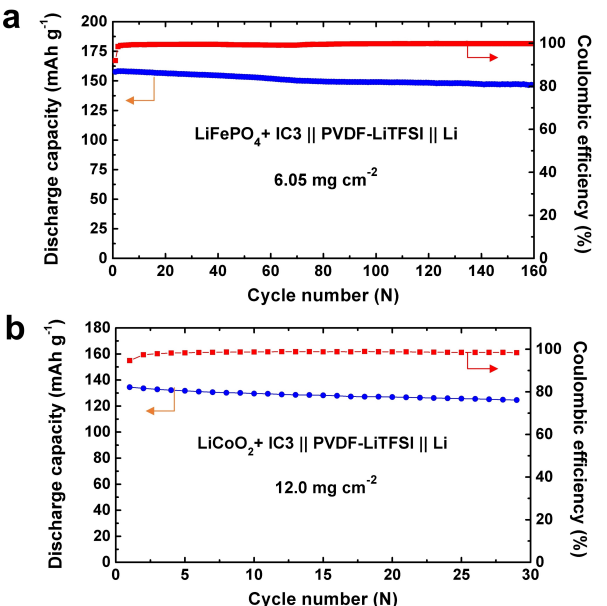


Figure 8. Cycle performance of the (a) $\text{LiFePO}_4 + \text{IC3} || \text{PVDF-LiTFSI} || \text{Li}$ cell and (b) $\text{LiCoO}_2 + \text{IC3} || \text{PVDF-LiTFSI} || \text{Li}$ cells with a high mass loading of active materials. The mass loadings are 6.05 and 12.0 mg cm^{-2} in (a) and (b), respectively.

literature and this work, especially those with SCN as an ionic conductor, and the cycle performance of the corresponding solid-state Li metal batteries. Our cells demonstrate excellent cycle performance due to the superior gel-like SCN- LiClO_4 ionic conductor.

3. Conclusions

Three kinds of SCN-based ICs with different flowability were synthesized and their behaviors in the composite cathodes of solid-state Li metal batteries were investigated. The flowable SCN-LiTFSI IC cannot be held in the composite cathode, while the rigid SCN- LiClO_4 IC cannot realize the stable interfacial contact, leading to the formation of micro-cracks in the cathode sheet; therefore, the interfacial resistance between the cathode and the electrolyte was significantly increased and the capacity of the batteries with these two ICs degraded quickly. By comparison, the gel-like SCN- LiClO_4 IC was useful to build an effective Li-ion conductive pathway in the composite cathodes

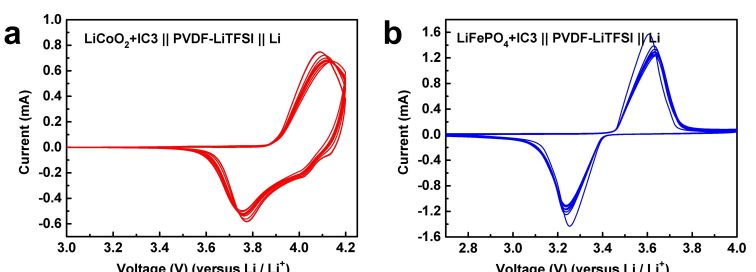


Figure 7. CV curves of the (a) LiCoO_2 and (b) LiFePO_4 cells with IC3-contained cathodes.

and buffer the volume change of cathode active particles. Thus, the solid-state batteries with the gel-like IC showed a small interfacial resistance after cycling and possessed a long cycle life. The experimental results show that it is critical to have a soft interfacial contact between the composite cathode and the polymer electrolyte, and the physical states of the ionic conductor in the composite cathode play an important role in the cycle performance of solid-state batteries. This work provides a guidance to design cathode additives for achieving a high mass loading of active materials and a stable cathode/electrolyte interface.

Experimental Section

For preparation of the composite cathode, LiFePO₄ or LiCoO₂ (Citic Guoan MGL Inc.), super P carbon black (TeenSky Inc.), poly(vinylidene fluoride) (PVDF, Arkema, Kynar 761) and LiTFSI (Sigma-Aldrich) with a weight ratio of 8:1:1:0.5 were first mixed in a *N*-methylpyrrolidone (NMP) solvent to form a slurry. The slurry was coated on an Al foil and dried in a vacuum oven at 110 °C for 12 h to obtain a cathode sheet. Three kinds of ionic conductors (ICs) were prepared by mixing SCN with LiTFSI or LiClO₄. SCN and LiTFSI with a molar ratio of 20:1 was homogeneously mixed by mechanical stirring for ~12 h at 80 °C. The resulting mixture, named IC1, was flowable at RT [Figure 9(a)]. SCN and LiClO₄ with a molar ratio of 20:1 was mixed by stirring for ~5 h at 80 °C to get a homogeneous solution and the resulting mixture, named IC2, was rigid and not flowable at RT [Figure 9(b)]. After IC2 stood for ~3 months, it was stirred again at 80 °C for ~20 h and the resulting product, named IC3, was gel-like after a period at RT [Figure 9(c)]. The viscosity of IC3 is much larger than that of IC1 in Figure S1 (Supporting Information), which is consistent with the corresponding photographs in Figure 9(a and c). Each IC was injected in the cathode sheet at 80 °C and the sheet surface was fully covered. The weight percentage of the IC in the cathode sheet was ~30–45 wt%. After the cathode sheet with the IC cooled down to RT, a composite cathode was obtained.

A CR2025 coin-type cell was assembled with the composite cathode containing a SCN-based ionic conductor, a PVDF-LiTFSI polymer electrolyte separator and a Li anode in an Ar-filled glovebox ($O_2 < 0.1$ ppm, $H_2O < 0.1$ ppm). The detailed preparation method of the PVDF-LiTFSI electrolyte membrane was reported as previously reported.^[7,45] No liquid electrolyte was added in these cells. The assembled cells were baked at 60 °C for a short time before use to optimize the interfacial contact between the composite cathode and the electrolyte separator.

The surface morphology of the SCN-based composite cathodes was analyzed by scanning electron microscopy (SEM, Zeiss Merlin) coupled with energy dispersive spectroscopy (EDS). The phase structure of the composite cathode was investigated by X-ray diffractometry (XRD, Rigaku D/max-2500 with Cu-K α at 40 kV and

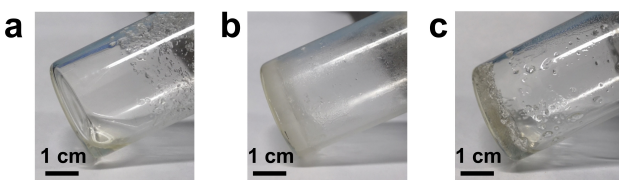


Figure 9. Photographs of SCN–Li salt ionic conductors. (a) Flowable IC1 (SCN–LiTFSI), (b) rigid IC2 (SCN–LiClO₄) and (c) gel-like IC3 (SCN–LiClO₄).

200 mA). The SCN–Li salt ICs were analyzed by Fourier transform infrared spectroscopy (FTIR, Bruker Tensor 27 spectrometer). Raman spectra (LabRAM HR800, HORIBA Jobin Yvon) were obtained with an excitation wavelength of 532 nm. The viscosity of the SCN-based ICs was measured by a modular compact rheometer (MCR302, Anton Paar) at 25 °C. The water content of the SCN-based ICs was tested by nuclear magnetic resonance (NMR, JNM-ECA600, JEOL). The impedance of the cells was measured by an impedance analyzer (ZAHNER-elektrik IM6) from 0.1 Hz to 8 MHz. The cyclic voltammetry (CV) measurement was performed by a potentiostat (Bio-Logic VMP3). The cycle performance of the cells was tested by a LANHE CT2001A battery testing system at 30 °C. The voltage ranges are 2.7 to 4.0 and 3.0 to 4.2 V for the LiFePO₄ and LiCoO₂ cells, respectively.

Supporting Information

Supporting Information is available from the Wiley Online Library or from the author.

Acknowledgements

This work was supported by the basic science center program of National Natural Science Foundation of China (Grant no. 51788104) and Tsinghua-Foshan Innovation Special Fund (Grant no. 2018THFS0409).

Conflict of Interest

The authors declare no conflict of interest.

Data Availability Statement

The raw/processed data required to reproduce the findings of this study are available from the corresponding author upon reasonable request.

Keywords: composite cathode • interfacial resistance • mass loading • succinonitrile • solid-state battery

- [1] L.-Z. Fan, H. He, C.-W. Nan, *Nat. Rev. Mater.* DOI: 10.1038/s41578-021-00320-0.
- [2] X. Zhang, T. Liu, S. Zhang, X. Huang, B. Xu, Y. Lin, B. Xu, L. Li, C. W. Nan, Y. Shen, *J. Am. Chem. Soc.* **2017**, *139*, 13779.
- [3] F. Lv, Z. Wang, L. Shi, J. Zhu, K. Edström, J. Mindemark, S. Yuan, *J. Power Sources* **2019**, *441*, 227175.
- [4] H. Huo, Y. Chen, J. Luo, X. Yang, X. Guo, X. Sun, *Adv. Energy Mater.* **2019**, *9*, 1804004.
- [5] Y.-X. Gong, J.-J. Wang, *Rare Met.* **2020**, *39*, 743.
- [6] L.-P. Wang, X.-D. Zhang, T.-S. Wang, Y.-X. Yin, J.-L. Shi, C.-R. Wang, Y.-G. Guo, *Adv. Energy Mater.* **2018**, *8*, 1801528.
- [7] C. Xin, X. Zhang, C. Xue, S. Wang, L. Li, C.-W. Nan, *Solid State Ionics* **2020**, *345*, 115196.
- [8] X. Chen, W. He, L.-X. Ding, S. Wang, H. Wang, *Energy Environ. Sci.* **2019**, *12*, 938.
- [9] R.-J. Chen, Y.-B. Zhang, T. Liu, B. Xu, Y. Shen, L. Li, Y.-H. Lin, C.-W. Nan, *Solid State Ionics* **2017**, *310*, 44.

- [10] A. I. Pitillas Martinez, F. Aguesse, L. Otaegui, M. Schneider, A. Roters, A. Llordés, L. Buannic, *J. Phys. Chem. C* **2019**, *123*, 3270.
- [11] H. Zeng, X. Ji, F. Tsai, Q. Zhang, T. Jiang, R. K. Y. Li, H. Shi, S. Luan, D. Shi, *Solid State Ionics* **2018**, *320*, 92.
- [12] X. Yang, Q. Sun, C. Zhao, X. Gao, K. R. Adair, Y. Liu, J. Luo, X. Lin, J. Liang, H. Huang, L. Zhang, R. Yang, S. Lu, R. Li, X. Sun, *Nano Energy* **2019**, *61*, 567.
- [13] J. C. Bachman, S. Muy, A. Grimaud, H. H. Chang, N. Pour, S. F. Lux, O. Paschos, F. Maglia, S. Lupart, P. Lamp, L. Giordano, Y. Shao-Horn, *Chem. Rev.* **2016**, *116*, 140.
- [14] B. Zhang, R. Tan, L. Yang, J. Zheng, K. Zhang, S. Mo, Z. Lin, F. Pan, *Energy Storage Mater.* **2018**, *10*, 139.
- [15] K. Park, B.-C. Yu, J.-W. Jung, Y. Li, W. Zhou, H. Gao, S. Son, J. B. Goodenough, *Chem. Mater.* **2016**, *28*, 8051.
- [16] T. Liu, Y. Zhang, R. Chen, S.-X. Zhao, Y. Lin, C.-W. Nan, Y. Shen, *Electrochem. Commun.* **2017**, *79*, 1.
- [17] J.-F. Wu, W. K. Pang, V. K. Peterson, L. Wei, X. Guo, *ACS Appl. Mater. Interfaces* **2017**, *9*, 12461.
- [18] F. Du, N. Zhao, Y. Li, C. Chen, Z. Liu, X. Guo, *J. Power Sources* **2015**, *300*, 24.
- [19] D. Dong, B. Zhou, Y. Sun, H. Zhang, G. Zhong, Q. Dong, F. Fu, H. Qian, Z. Lin, D. Lu, Y. Shen, J. Wu, L. Chen, H. Chen, *Nano Lett.* **2019**, *19*, 2343.
- [20] Z. Lu, J. Yu, J. Wu, M. B. Effat, S. C. T. Kwok, Y. Lyu, M. M. F. Yuen, F. Ciucci, *Energy Storage Mater.* **2019**, *18*, 311.
- [21] M. He, Z. Cui, F. Han, X. Guo, *J. Alloys Compd.* **2018**, *762*, 157.
- [22] B. Hu, W. Yu, B. Xu, X. Zhang, T. Liu, Y. Shen, Y. H. Lin, C. W. Nan, L. Li, *ACS Appl. Mater. Interfaces* **2019**, *11*, 34939.
- [23] Y. Li, B. Xu, H. Xu, H. Duan, X. Lu, S. Xin, W. Zhou, L. Xue, G. Fu, A. Manthiram, J. B. Goodenough, *Angew. Chem. Int. Ed.* **2017**, *56*, 753.
- [24] D. Zhou, Y.-B. He, R. Liu, M. Liu, H. Du, B. Li, Q. Cai, Q.-H. Yang, F. Kang, *Adv. Energy Mater.* **2015**, *5*, 1500353.
- [25] Z. Zhao, Y. Zhang, S. Li, S. Wang, Y. Li, H. Mi, L. Sun, X. Ren, P. Zhang, *J. Mater. Chem. A* **2019**, *7*, 25818.
- [26] X. Wang, Y. Zhang, X. Zhang, T. Liu, Y. H. Lin, L. Li, Y. Shen, C. W. Nan, *ACS Appl. Mater. Interfaces* **2018**, *10*, 24791.
- [27] L.-Z. Fan, J. Maier, *Electrochem. Commun.* **2006**, *8*, 1753.
- [28] K. Liu, Q. Zhang, B. P. Thapaliya, X.-G. Sun, F. Ding, X. Liu, J. Zhang, S. Dai, *Solid State Ionics* **2020**, *345*, 115159.
- [29] H. M. Bintang, S. Lee, S. Shin, B. G. Kim, H.-G. Jung, D. Whang, H.-D. Lim, *Chem. Eng. J.* **2021**, *424*, 130524.
- [30] Z. Wei, S. Chen, J. Wang, Z. Wang, Z. Zhang, X. Yao, Y. Deng, X. Xu, *J. Power Sources* **2018**, *394*, 57.
- [31] M. Falco, S. Ferrari, G. B. Appetecchi, C. Gerbaldi, *Mol. Syst. Des. Eng.* **2019**, *4*, 850.
- [32] Y. Y. Sun, Y. Y. Wang, G. R. Li, S. Liu, X. P. Gao, *ACS Appl. Mater. Interfaces* **2019**, *11*, 14830.
- [33] J. Y. Liang, X. X. Zeng, X. D. Zhang, P. F. Wang, J. Y. Ma, Y. X. Yin, X. W. Wu, Y. G. Guo, L. J. Wan, *J. Am. Chem. Soc.* **2018**, *140*, 6767.
- [34] M. B. Dixit, W. Zaman, N. Hortance, S. Vujić, B. Harkey, F. Shen, W.-Y. Tsai, V. De Andrade, X. C. Chen, N. Balke, K. B. Hatzell, *Joule* **2020**, *4*, 207.
- [35] J. Zhang, N. Zhao, M. Zhang, Y. Li, P. K. Chu, X. Guo, Z. Di, X. Wang, H. Li, *Nano Energy* **2016**, *28*, 447.
- [36] T. Jiang, P. He, G. Wang, Y. Shen, C. W. Nan, L. Z. Fan, *Adv. Energy Mater.* **2020**, *10*, 1903376.
- [37] Y.-C. Jung, M.-S. Park, C.-H. Doh, D.-W. Kim, *Electrochim. Acta* **2016**, *218*, 271.
- [38] B. Zhang, L. Chen, J. Hu, Y. Liu, Y. Liu, Q. Feng, G. Zhu, L.-Z. Fan, *J. Power Sources* **2019**, *442*, 227230.
- [39] J. Hu, P. He, B. Zhang, B. Wang, L. Z. Fan, *Energy Storage Mater.* **2020**, *26*, 283.
- [40] B. Liu, L. Zhang, S. Xu, D. W. McOwen, Y. Gong, C. Yang, G. R. Pastel, H. Xie, K. Fu, J. Dai, C. Chen, E. D. Wachsman, L. Hu, *Energy Storage Mater.* **2018**, *14*, 376.
- [41] C. Wang, Q. Sun, Y. Liu, Y. Zhao, X. Li, X. Lin, M. N. Banis, M. Li, W. Li, K. R. Adair, D. Wang, J. Liang, R. Li, L. Zhang, R. Yang, S. Lu, X. Sun, *Nano Energy* **2018**, *48*, 35.
- [42] P.-J. Alarco, Y. Abu-Lebdeh, A. Abouimrane, M. Armand, *Nat. Mater.* **2004**, *3*, 476.
- [43] M. B. Effat, Z. Lu, A. Belotti, J. Yu, Y.-Q. Lyu, F. Ciucci, *J. Power Sources* **2019**, *436*, 226802.
- [44] C.-Z. Zhao, B.-C. Zhao, C. Yan, X.-Q. Zhang, J.-Q. Huang, Y. Mo, X. Xu, H. Li, Q. Zhang, *Energy Storage Mater.* **2020**, *24*, 75.
- [45] X. Zhang, S. Wang, C. Xue, C. Xin, Y. Lin, Y. Shen, L. Li, C. W. Nan, *Adv. Mater.* **2019**, *31*, 1806082.
- [46] W. Yang, X. Du, J. Zhao, Z. Chen, J. Li, J. Xie, Y. Zhang, Z. Cui, Q. Kong, Z. Zhao, C. Wang, Q. Zhang, G. Cui, *Joule* **2020**, *4*, 1557.
- [47] Q. Wang, H. Fan, L.-Z. Fan, Q. Shi, *Electrochim. Acta* **2013**, *114*, 720.
- [48] Z. Hu, F. Xian, Z. Guo, C. Lu, X. Du, X. Cheng, S. Zhang, S. Dong, G. Cui, L. Chen, *Chem. Mater.* **2020**, *32*, 3405.
- [49] W. Huang, S. Zheng, X. Zhang, W. Zhou, W. Xiong, J. Chen, *Energy Storage Mater.* **2020**, *26*, 465.

Manuscript received: July 12, 2021

Revised manuscript received: August 31, 2021

Accepted manuscript online: September 7, 2021

Version of record online: September 24, 2021